

SOLID-LIQUID PHASE EQUILIBRIUM: ALKANE SYSTEMS FOR LOW TEMPERATURE ENERGY STORAGE

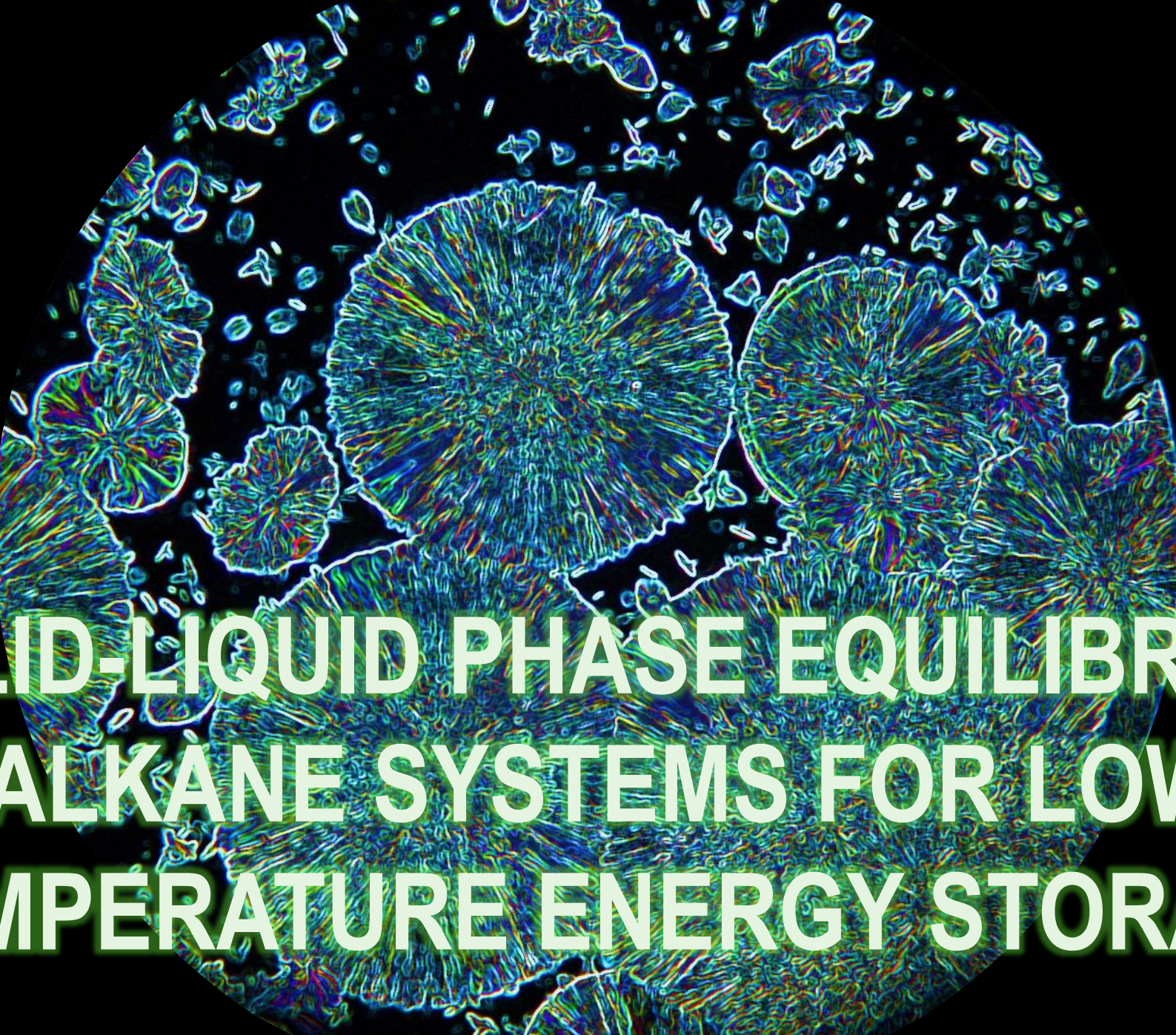
Maria C. M. Sequeira¹, Bernardo A. Nogueira², Fernando J. P. Caetano^{1,3}, Hermínio A. P. Diogo¹, João M. N. A. Fareleira¹, Rui Fausto^{2,4}

¹*Centro de Química Estrutural Institute of Molecular Sciences (IMS), Univ. Lisboa, Portugal*

²*Centro de Química de Coimbra Institute of Molecular Sciences (IMS), Dept. de Química, Univ. Coimbra, Portugal*

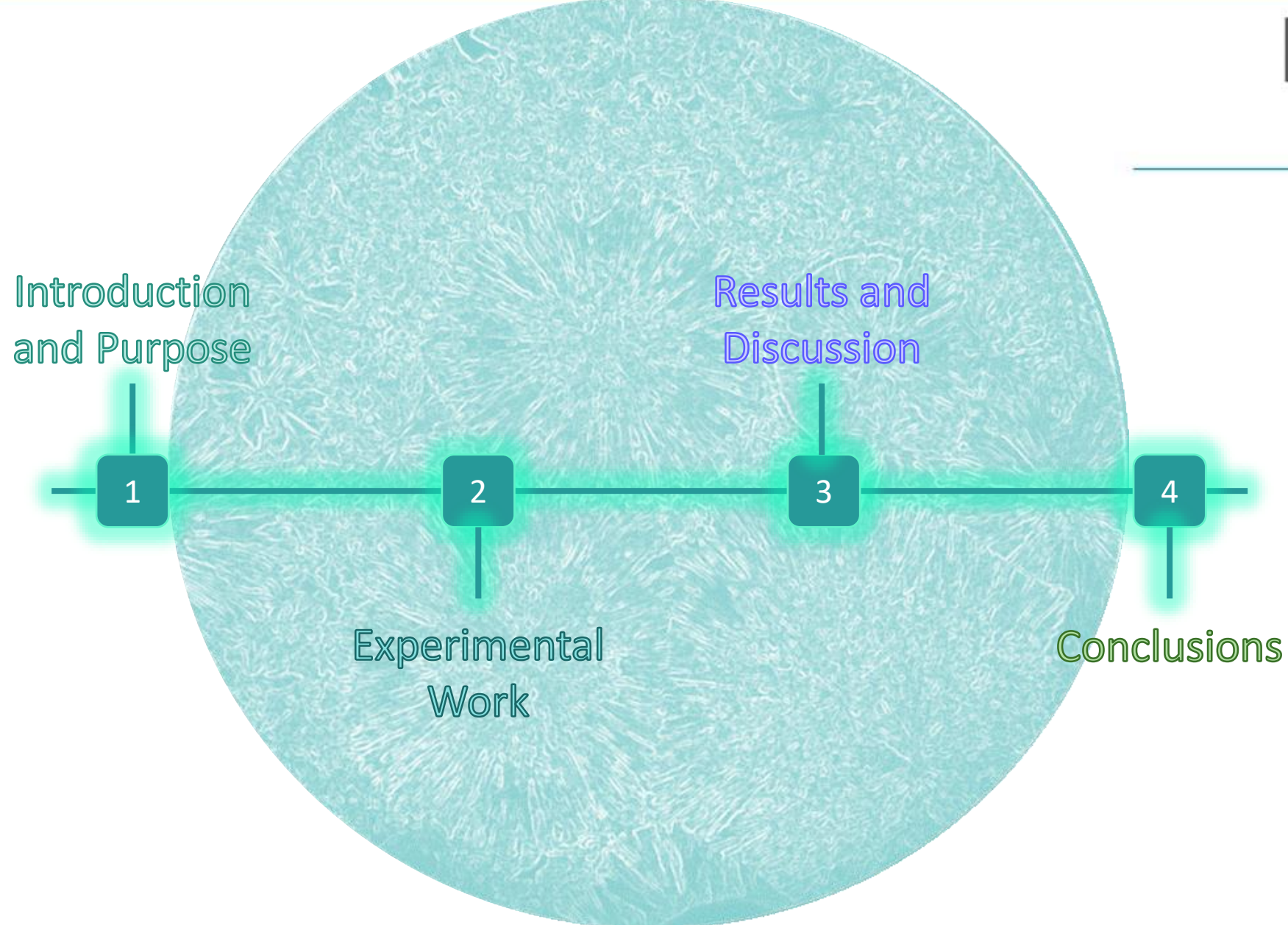
³*Departamento de Ciências e Tecnologia, Univ. Aberta, Portugal*

⁴*Faculty of Sciences and Letters, Dept. of Physics, Istanbul Kultur Univ., Ataköy Campus, Bakırköy 34156, Istanbul, Turkey*



A polarized light micrograph showing large, well-defined spherulitic crystal structures of alkanes. These structures exhibit a radial, fibrous texture with distinct color fringes, primarily in shades of blue, green, and yellow. Smaller, more irregular crystalline fragments are scattered throughout the field.

SOLID-LIQUID PHASE EQUILIBRIUM: ALKANE SYSTEMS FOR LOW TEMPERATURE ENERGY STORAGE



1. INTRODUCTION AND PURPOSE

Increasing Energy Needs



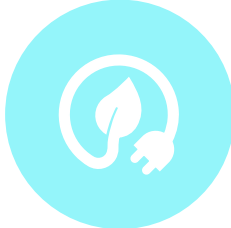
Fossil Fuels



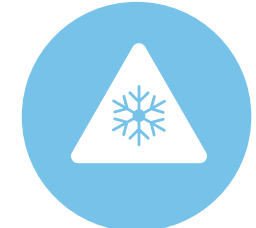
PCMs and Eutectics



Renewable Energies



Low Temperature Energy Storage



Gap between supply and consumption

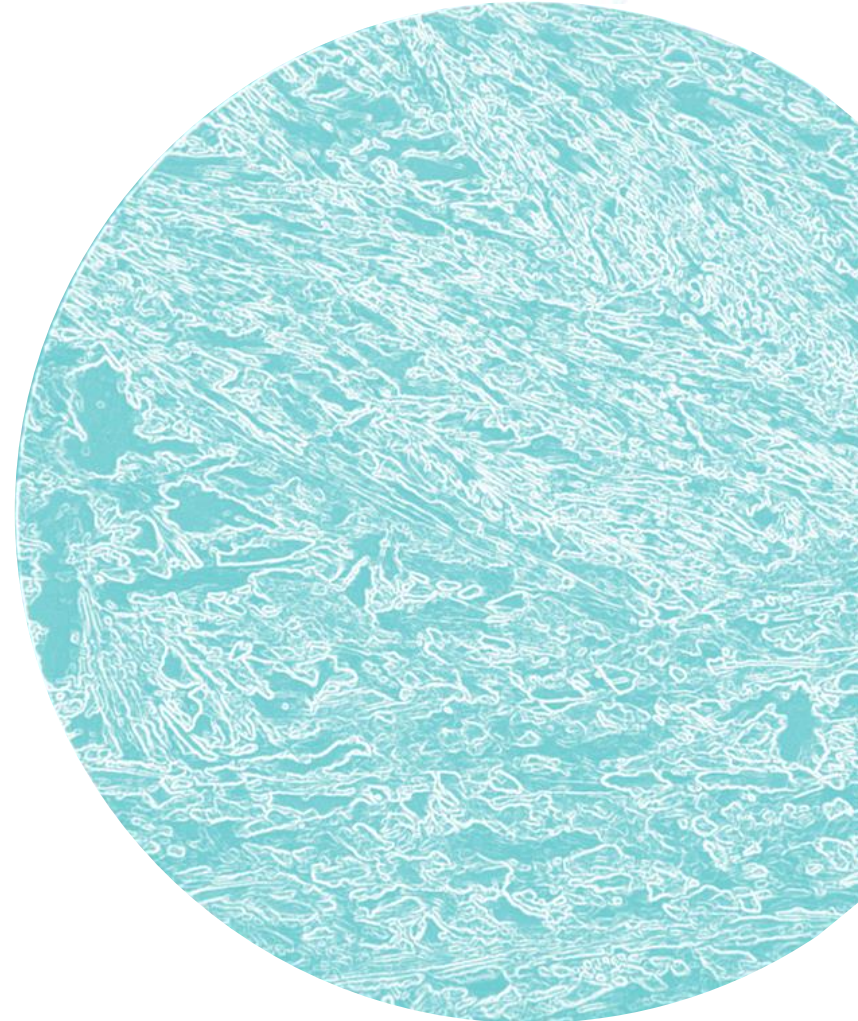


Energy Storage as solution

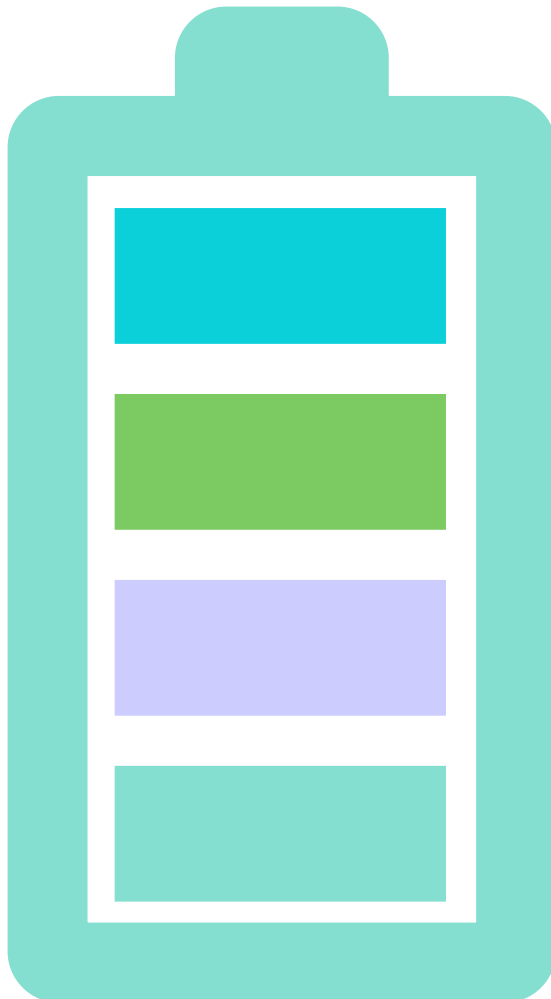


1. INTRODUCTION AND PURPOSE

Characterization of selected systems that can be used for thermal energy storage at low temperatures to understand their behaviour and robustness as PCMs



2. EXPERIMENTAL WORK



Construction of the Solid – Liquid Binary Phase Diagrams



Low Temperature Raman Spectroscopy



Differential Scanning Calorimetry experiments (DSC)



Binary Systems:

$n\text{-octane (C}_8\text{)} + n\text{-decane (C}_{10}\text{)}$

$n\text{-decane (C}_{10}\text{)} + n\text{-dodecane (C}_{12}\text{)}$

3. RESULTS AND DISCUSSION

*Preliminary results

DSC RESULTS

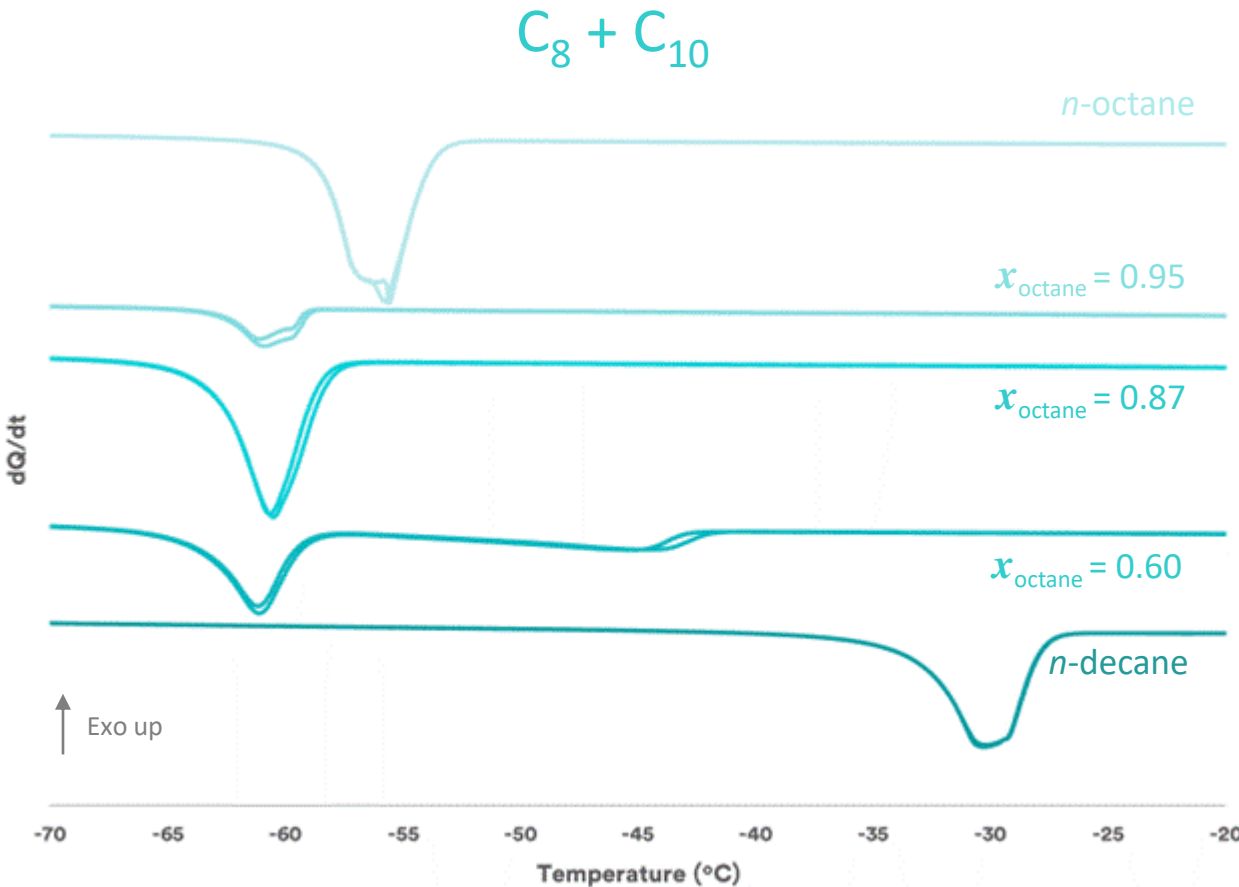


Fig. 1 – DSC heating curves of pure n-octane, n-decane, and of selected binary mixtures, with octane molar fraction x_{octane} .

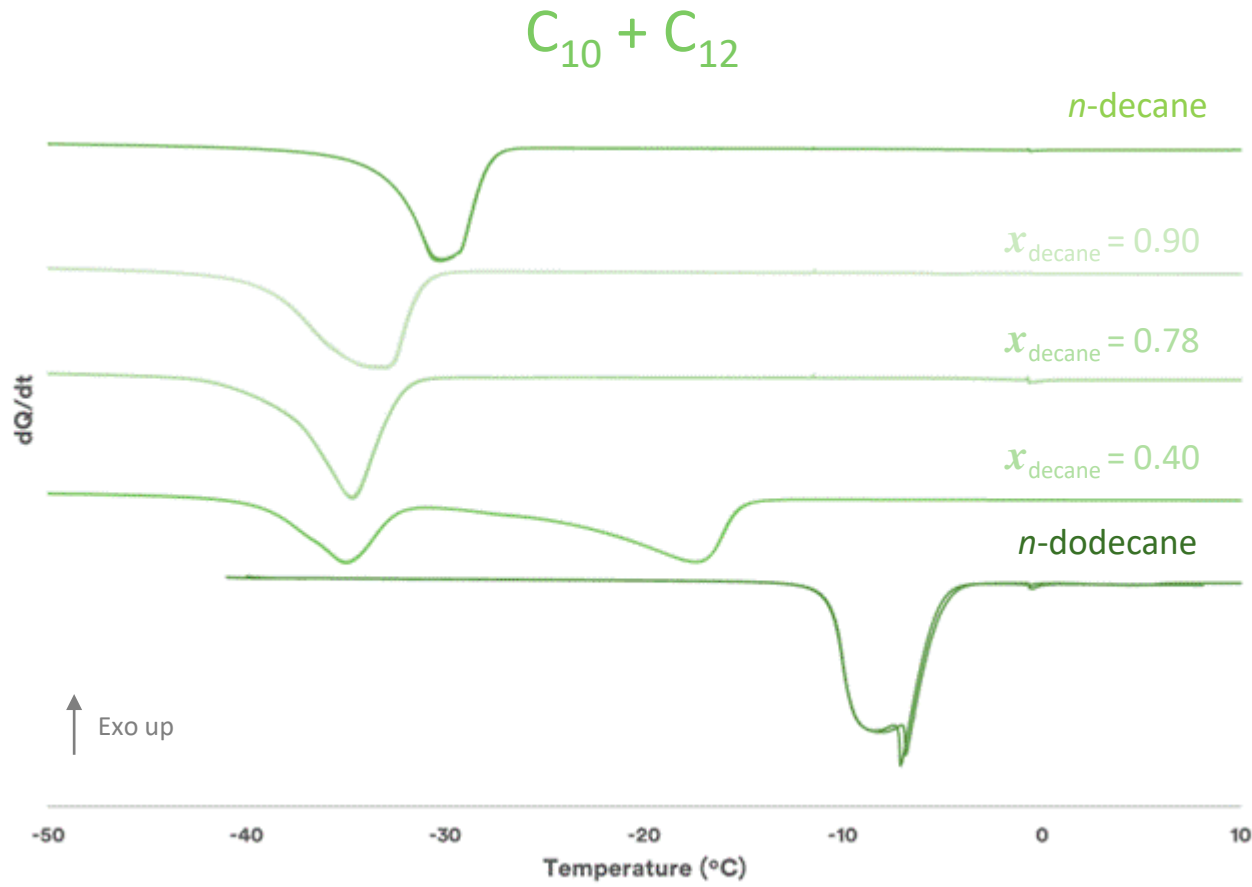


Fig. 2 – DSC heating curves of pure n-decane, n-dodecane, and of selected binary mixtures, with octane molar fraction x_{decane} .

DSC RESULTS

For pure compounds and eutectic mixtures: only a single peak for the phase transition

For other binary mixtures: two peaks for the phase transition

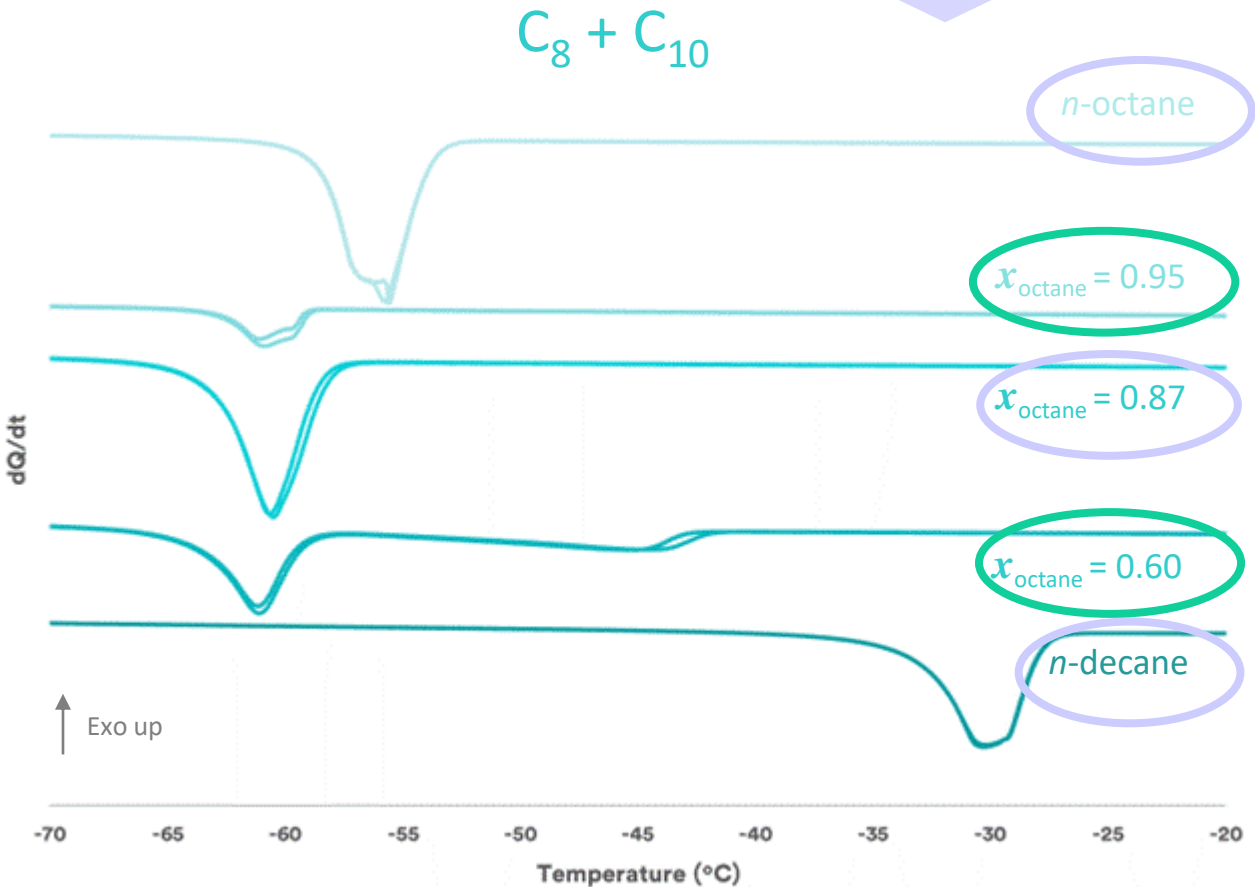


Fig. 1 – DSC heating curves of pure *n*-octane, *n*-decane, and of selected binary mixtures, with octane molar fraction x_{octane} .

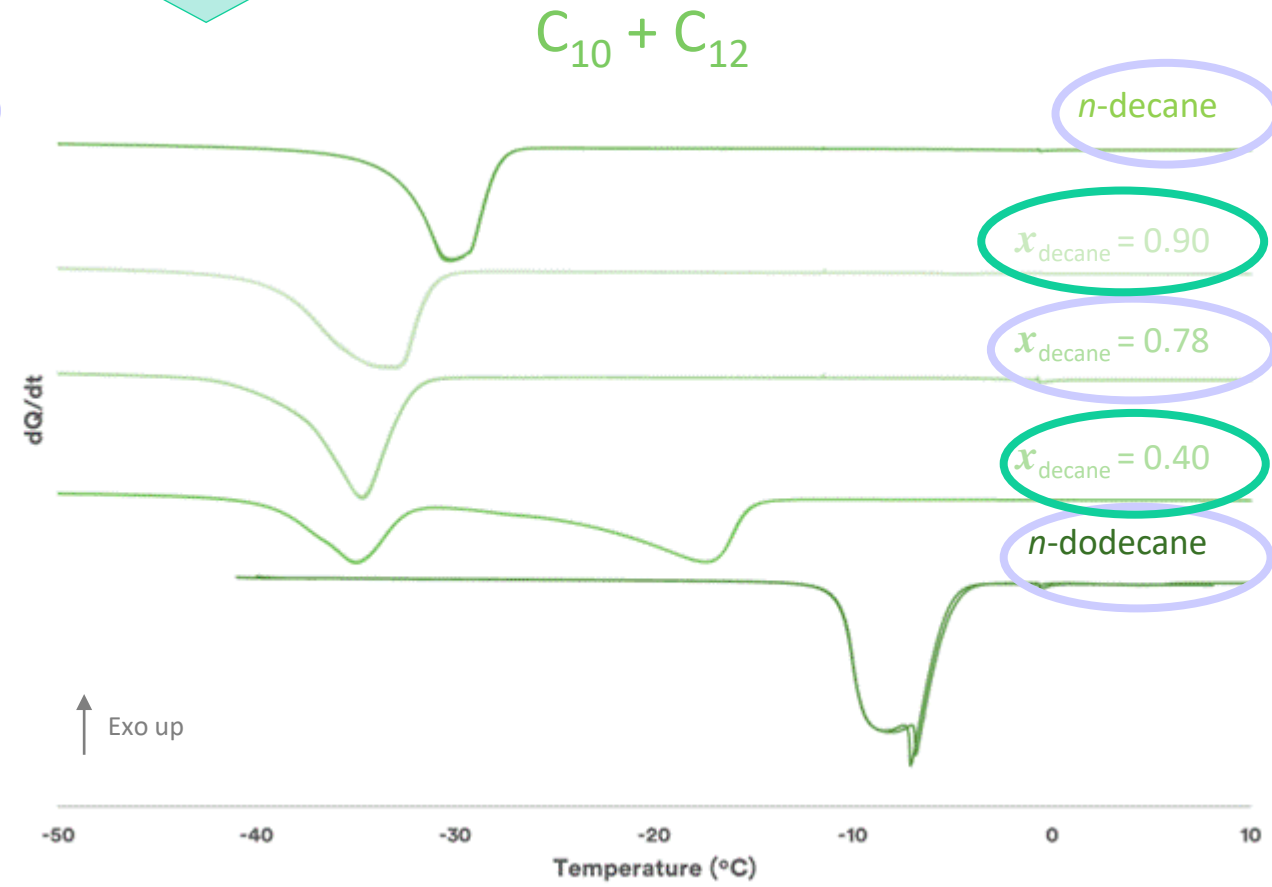
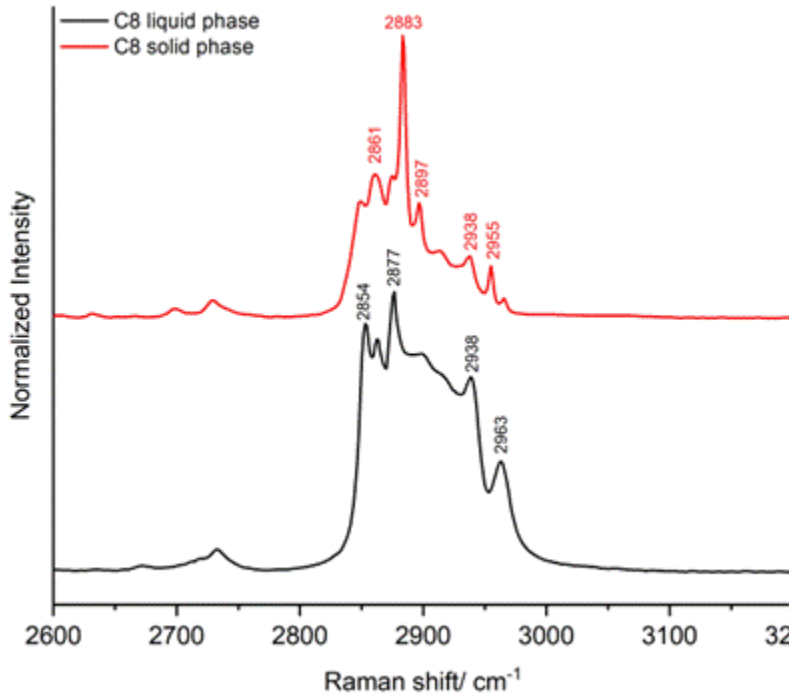


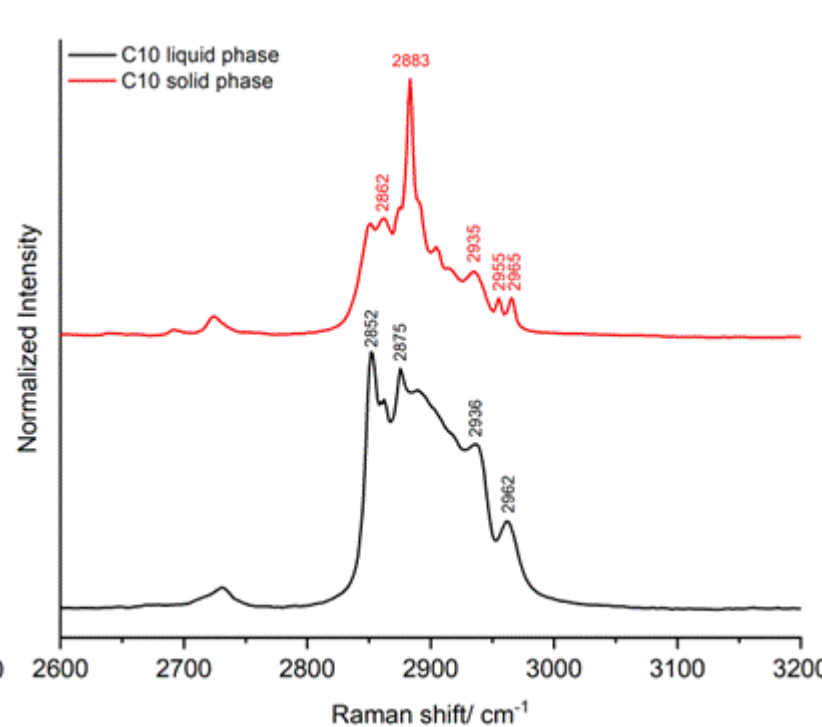
Fig. 2 – DSC heating curves of pure *n*-decane, *n*-dodecane, and of selected binary mixtures, with octane molar fraction x_{decane} .

RAMAN SPECTROSCOPY

C₈



C₁₀



C₁₂

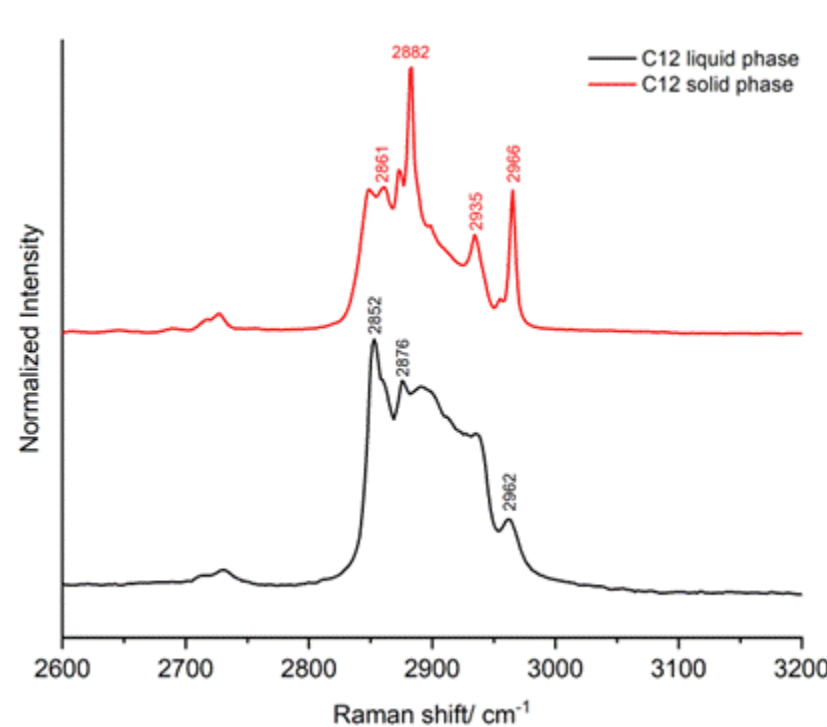
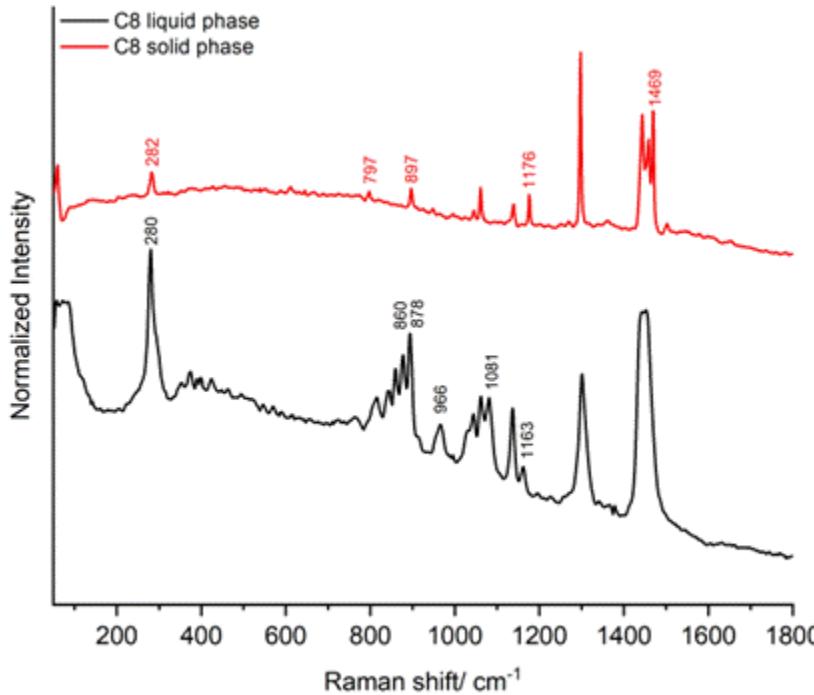


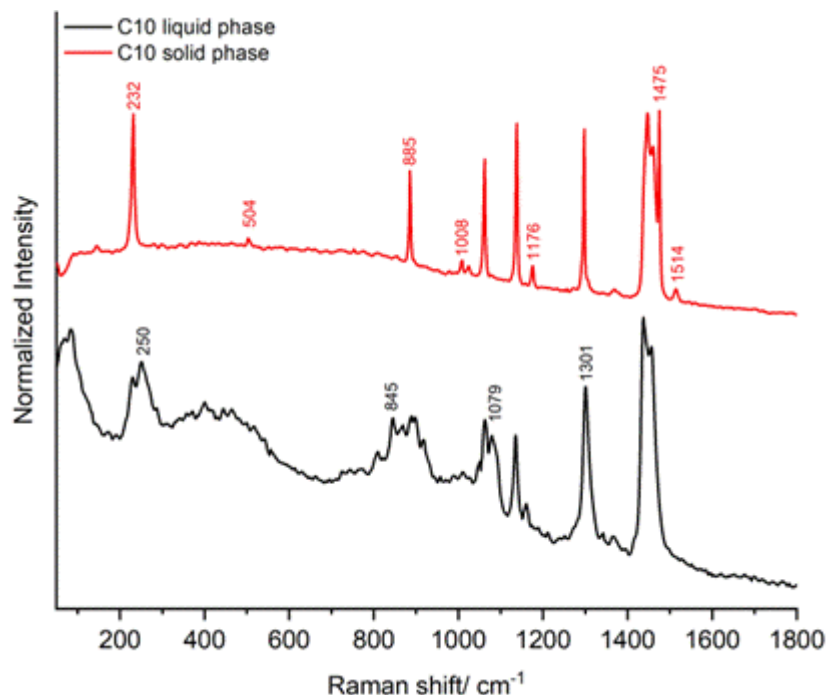
Fig. 3 – Raman spectra of room-temperature liquid phase and cooled solid phase samples of C₈, C₁₀ and C₁₂, with marker bands in the 2600-3200 cm⁻¹ range.

RAMAN SPECTROSCOPY

C_8



C_{10}



C_{12}

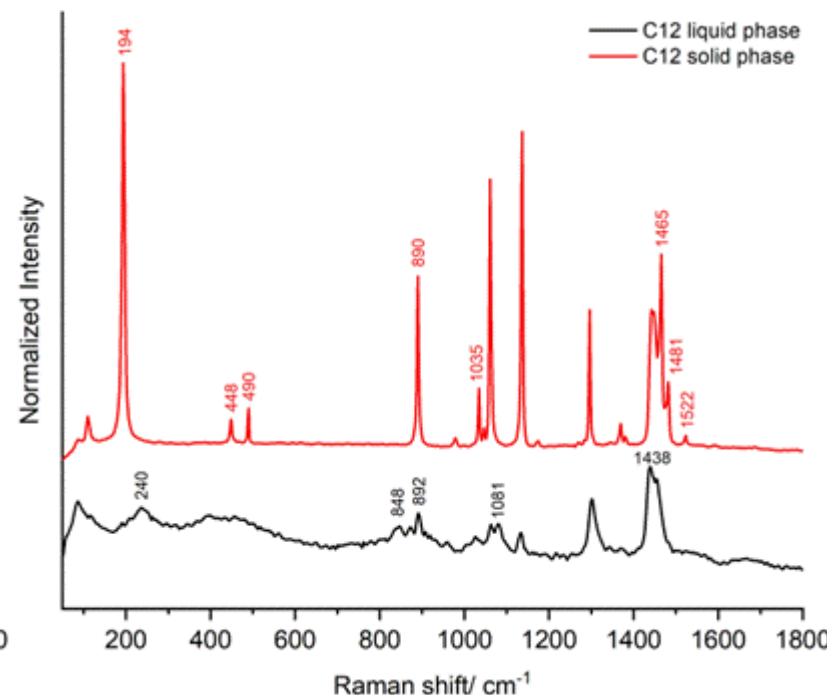


Fig. 4 – Raman spectra of room-temperature liquid phase and cooled solid phase samples of C_8 , C_{10} and C_{12} , with marker bands in the 50-1800 cm^{-1} range.

RAMAN SPECTROSCOPY

ECTP 2023
Venice ITALY
10-13 September 2023

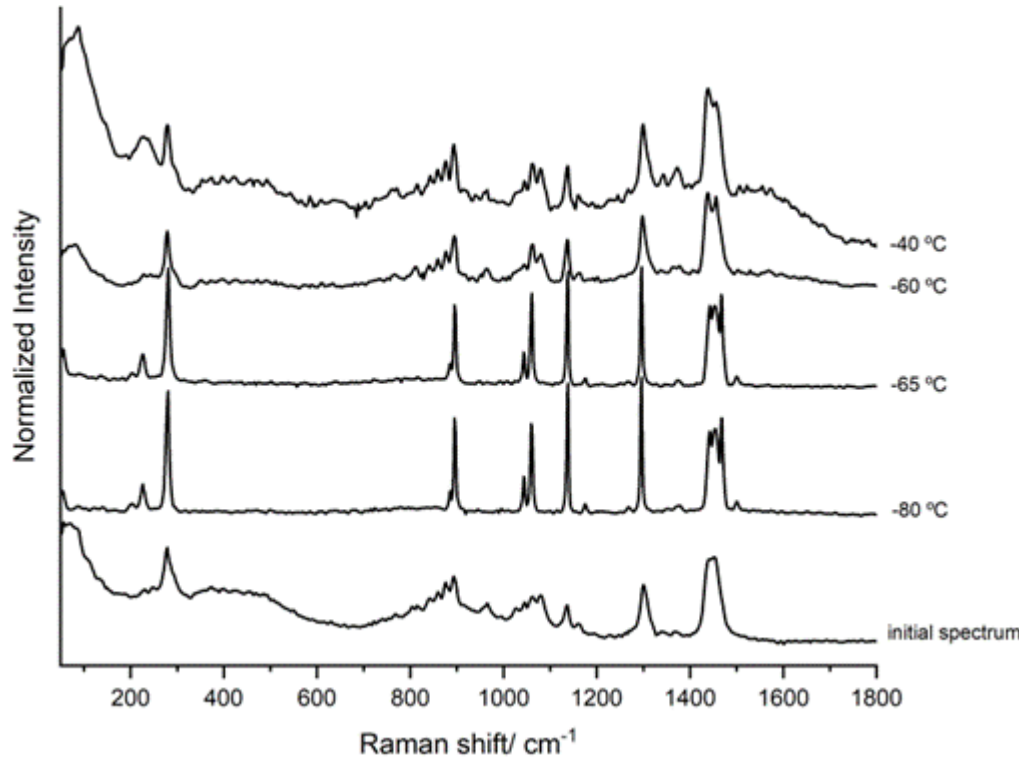


Fig. 5 – Temperature-variation Raman spectra of the 87:13 C₈-C₁₀ binary system.

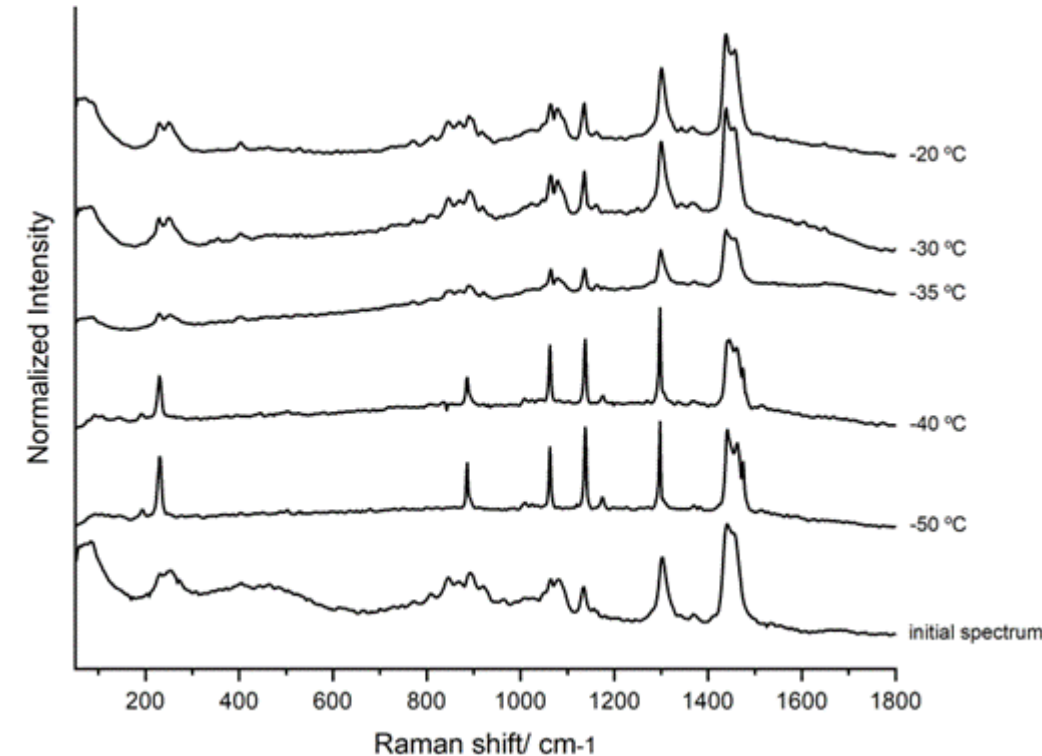


Fig. 6 – Temperature-variation Raman spectra of the 78:22 C₁₀-C₁₂ binary system.

BINARY PHASE DIAGRAM

$C_8 + C_{10}$

Mondieig* et al. 2004 (DOI: 10.1021/cm031169p)

- ✓ Eutectic Behaviour
- ✓ Eutectic Temperature
- ✓ Eutectic Composition
- ✓ Temperature values

- ✗ Enthalpy values ✗
- ✗ $C_{10} + C_{12}$ system ✗

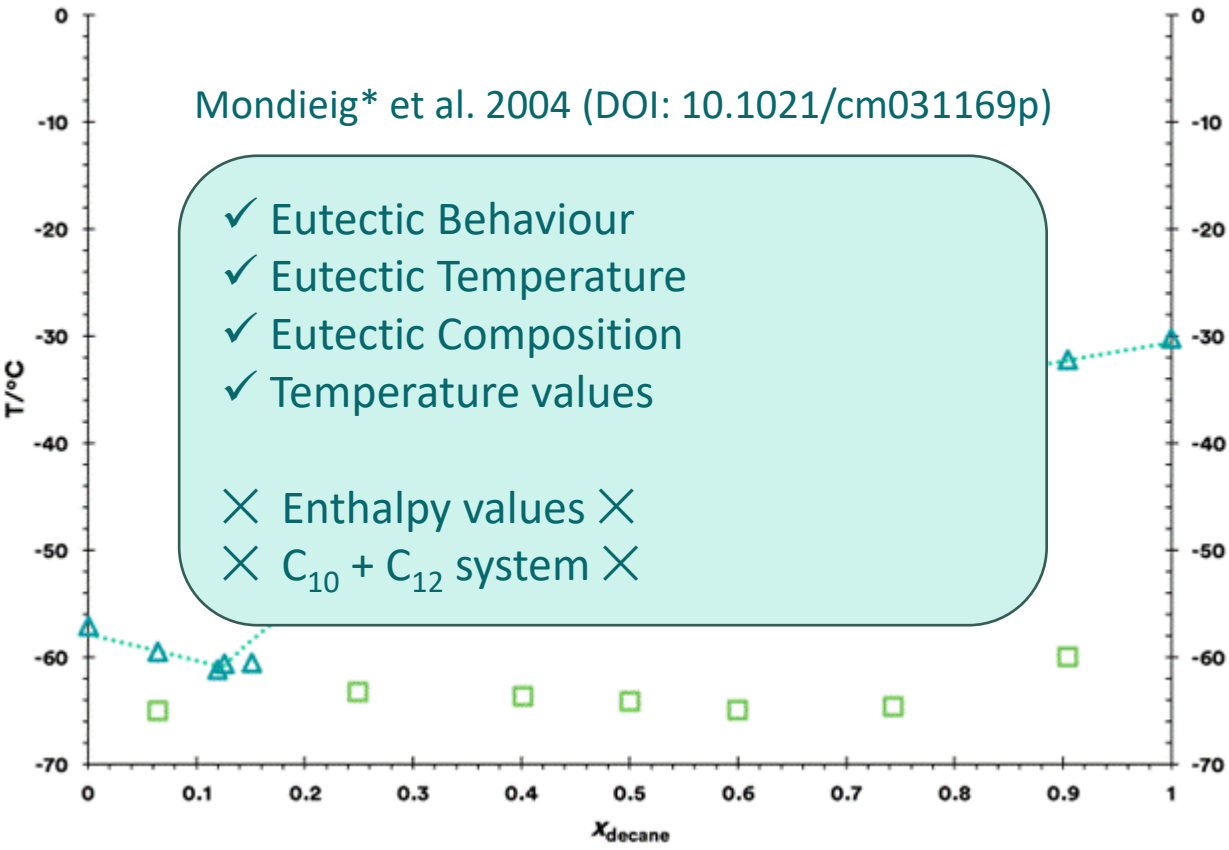


Fig. 7 – Binary solid-liquid phase diagram of *n*-octane and *n*-decane.

$C_{10} + C_{12}$

Ventolà* et al. 2002 (DOI: 10.1007/s10019-002-0213-3)

- ✓ Eutectic Behaviour
- ± Eutectic Temperature
- ± Eutectic Composition

- ✗ Temperature ✗
- ✗ Enthalpy values ✗

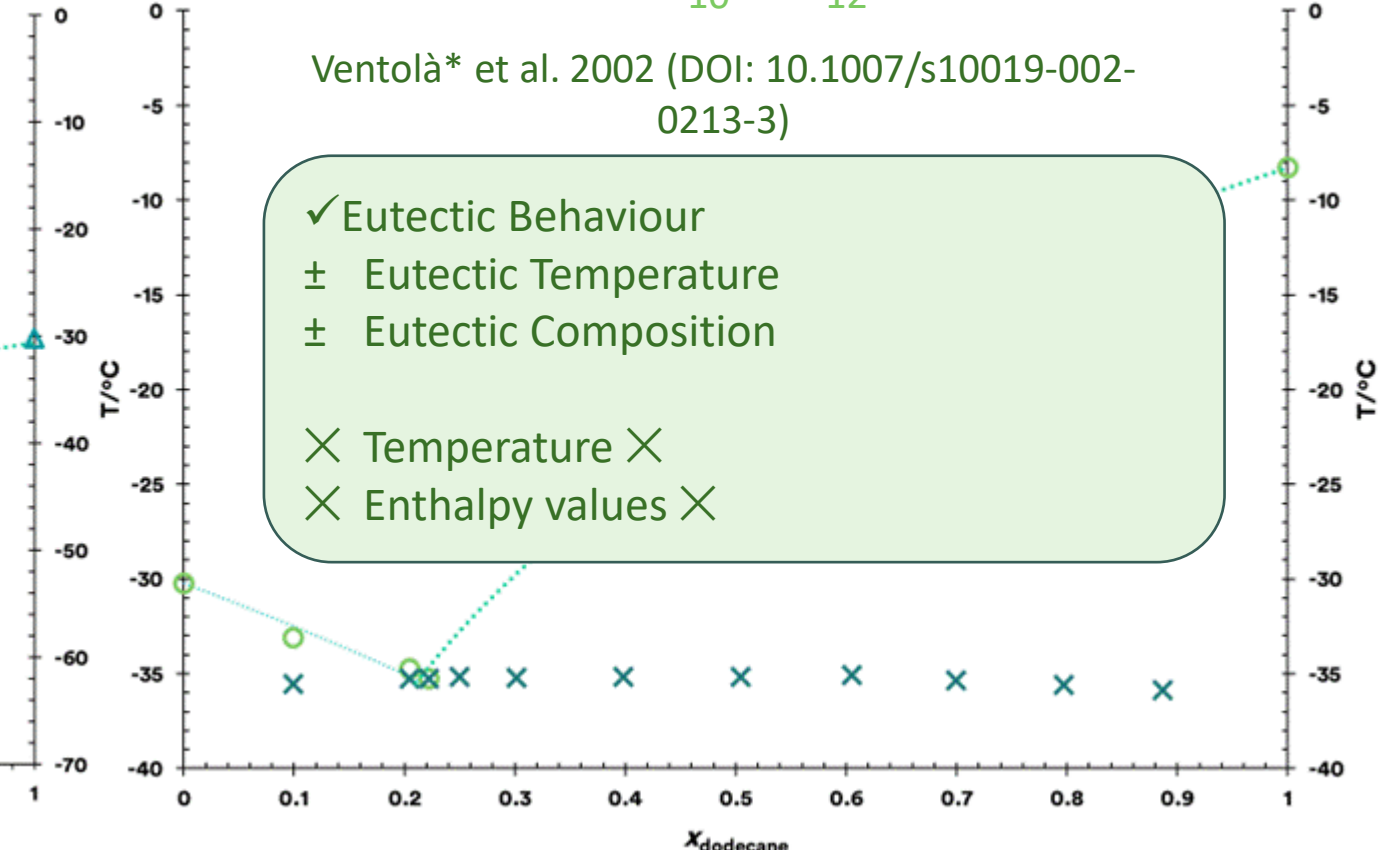


Fig. 8 – Binary solid-liquid phase diagram of *n*-decane and *n*-dodecane.

BINARY PHASE DIAGRAM

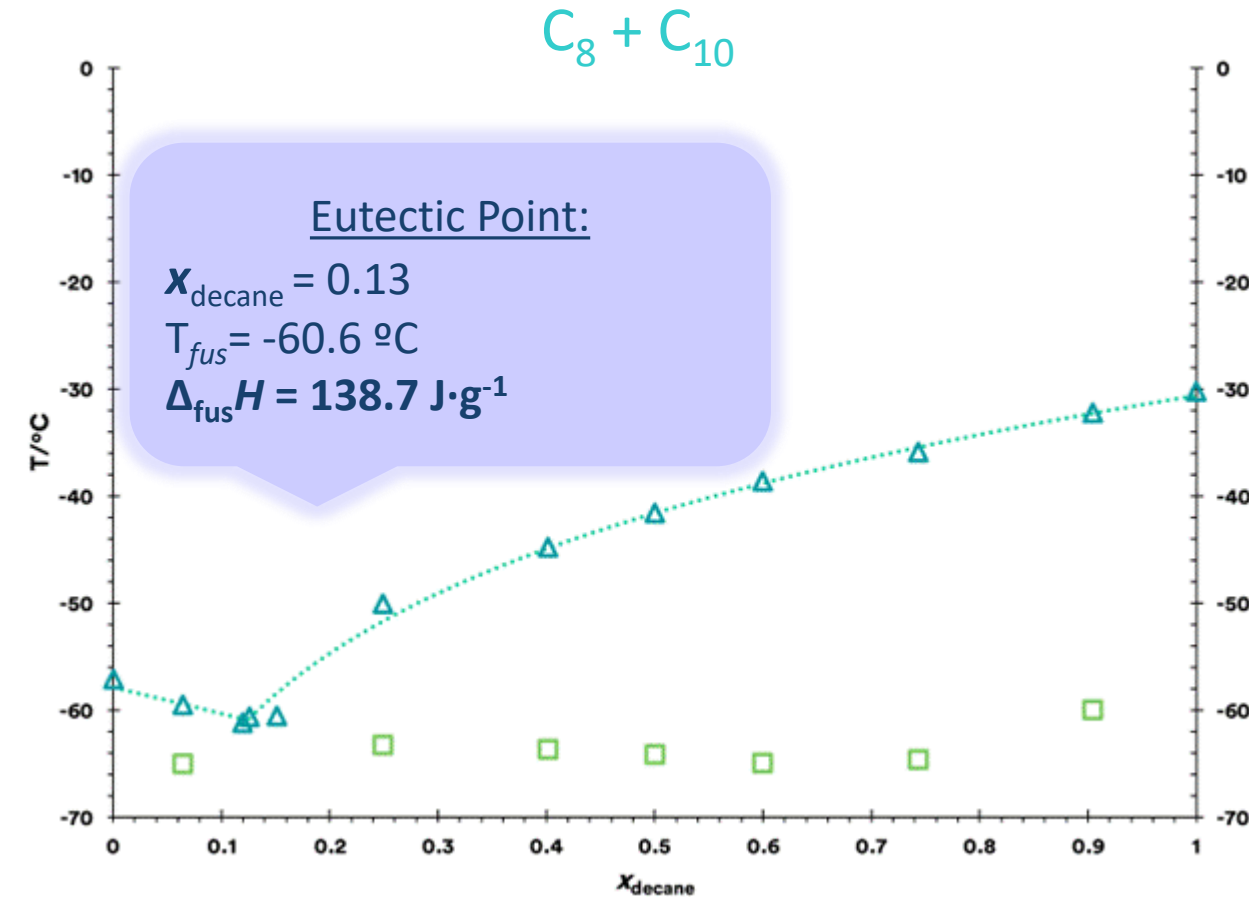


Fig. 7 – Binary solid-liquid phase diagram of *n*-octane and *n*-decane.

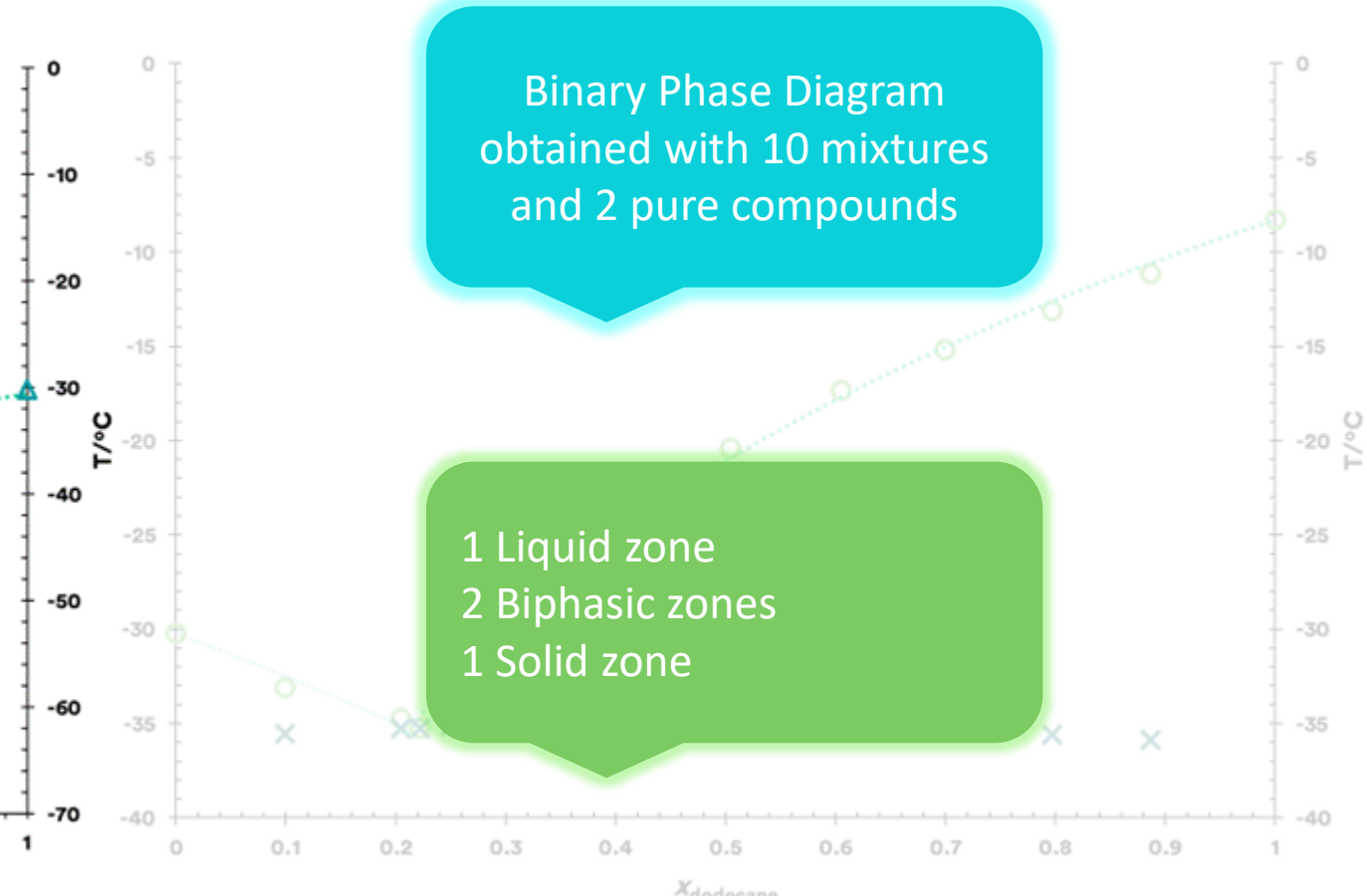


Fig. 8 – Binary solid-liquid phase diagram of *n*-decane and *n*-dodecane.

BINARY PHASE DIAGRAM

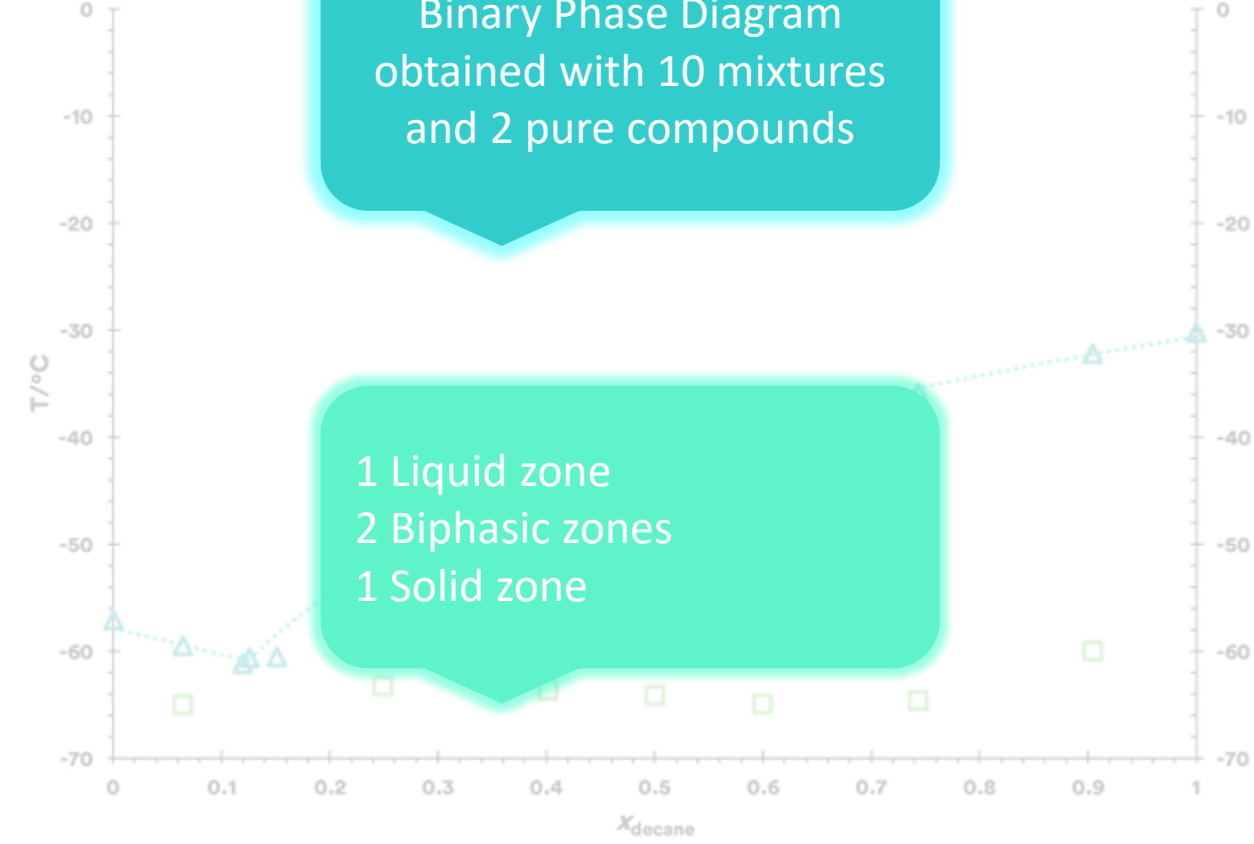


Fig. 7 – Binary solid-liquid phase diagram of *n*-octane and *n*-decane.

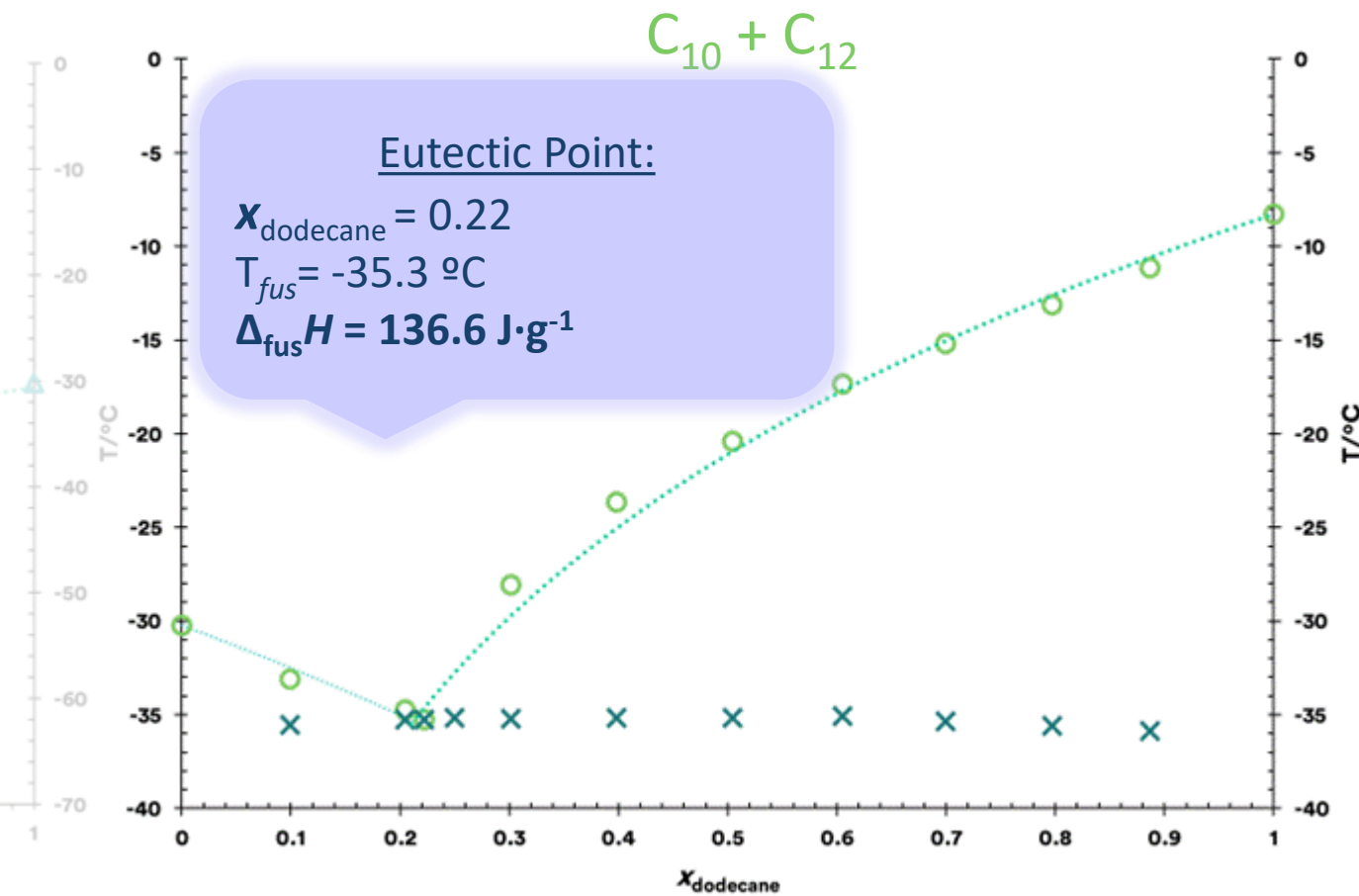


Fig. 8 – Binary solid-liquid phase diagram of *n*-decane and *n*-dodecane.

BINARY PHASE DIAGRAM - FITTING

Freezing-point depression curve¹

$$\ln\left(\frac{1}{x}\right) = \frac{L_{Mi}}{R} \left(\frac{1}{T} - \frac{1}{T_{Mi}} \right)$$

$$\ln\left(\frac{1}{x}\right) = a + b \cdot \frac{1}{T}$$

Fitting Parameters

$$a = -\frac{L_{Mi}}{R} \cdot \frac{1}{T_{Mi}} ; \quad b = \frac{L_{Mi}}{R}$$

Binary Phase Diagram $C_8 + C_{10}$

Table 1 – Comparison of the experimental results with the fitting results for the pure compounds *n*-octane and *n*-decane.

<i>n</i> -octane			<i>n</i> -decane		
$L_{Mi}/\text{kJ}\cdot\text{mol}^{-1}$	$\Delta_{\text{fus}}H/\text{kJ}\cdot\text{mol}^{-1}$	Dev./ $\text{kJ}\cdot\text{mol}^{-1}$	$L_{Mi}/\text{kJ}\cdot\text{mol}^{-1}$	$\Delta_{\text{fus}}H/\text{kJ}\cdot\text{mol}^{-1}$	Dev./ $\text{kJ}\cdot\text{mol}^{-1}$
16.7	21.4	4.7	29.5	24.1	5.4
$T_{Mi}/^\circ\text{C}$	$T_{\text{fus}}/^\circ\text{C}$	Dev./ $^\circ\text{C}$	$T_{Mi}/^\circ\text{C}$	$T_{\text{fus}}/^\circ\text{C}$	Dev./ $^\circ\text{C}$
-57.9	-57.1	0.8	-30.6	-30.2	0.4
Eutectic Point					
$x_{\text{decane}} \text{ (exp.)}$	$x_{\text{decane}} \text{ (fit)}$	$T_{\text{exp}}/^\circ\text{C}$	$T_{\text{fit}}/^\circ\text{C}$	Dev./ $^\circ\text{C}$	
0.126	0.126	-60.6	-60.9	0.3	

Maximum absolute deviation for all data: $\pm 2.2 \text{ } ^\circ\text{C}$

¹K. Denbigh, Principles of Chemical Equilibrium, 2nd Ed. London, United Kingdom: Cambridge University Press, 1966.

BINARY PHASE DIAGRAM - FITTING

Freezing-point depression curve¹

$$\ln\left(\frac{1}{x}\right) = \frac{L_{Mi}}{R} \left(\frac{1}{T} - \frac{1}{T_{Mi}} \right)$$

$$\ln\left(\frac{1}{x}\right) = a + b \cdot \frac{1}{T}$$

Fitting Parameters

$$a = -\frac{L_{Mi}}{R} \cdot \frac{1}{T_{Mi}} ; \quad b = \frac{L_{Mi}}{R}$$

Binary Phase Diagram C₁₀ + C₁₂

Table 2 – Comparison of the experimental results with the fitting results for the pure compounds n-decane and n-dodecane.

n-decane			n-dodecane		
L _{Mi} /kJ·mol ⁻¹	Δ _{fus} H/kJ·mol ⁻¹	Dev./kJ·mol ⁻¹	L _{Mi} /kJ·mol ⁻¹	Δ _{fus} H/kJ·mol ⁻¹	Dev./kJ·mol ⁻¹
22.4	24.1	1.7	30.0	34.3	4.3
T _{Mi} /°C	T _{fus} /°C	Dev./°C	T _{Mi} /°C	T _{fus} /°C	Dev./°C
-30.4	-30.2	0.2	-8.4	-8.3	0.1
Eutectic Point					
x _{dodecane} (exp.)	x _{dodecane} (fit.)	T _{exp} /°C	T _{fit} /°C	Dev./°C	
0.221	0.193	-35.3	-35.2	0.1	

Maximum absolute deviation for all data: ±0.9 °C

¹K. Denbigh, Principles of Chemical Equilibrium, 2nd Ed. London, United Kingdom: Cambridge University Press, 1966.

4. CONCLUSIONS

Two studied systems of *n*-alkanes:

- *n*-octane C₈ + *n*-decane C₁₀
- *n*-decane C₁₀ + *n*-dodecane C₁₂

Solid-liquid binary phase diagrams:

- Eutectic Systems
- Fitting of the liquidus line

Experimental Techniques:

- DSC
- Raman Spectroscopy

Potential PCMs for low Temp. ES:

- C₈/C₁₀: T_{fus} = -60.6 °C; Δ_{fus}H = 138.7 J·g⁻¹
- C₁₀/C₁₂: T_{fus} = -35.3 °C; Δ_{fus}H = 136.6 J·g⁻¹

ACKNOWLEDGMENTS

ECTP 2023
Venice ITALY
10-13 September 2023

This work was supported by Fundação para a Ciência e a Tecnologia (FCT), Portugal, Projects UIDB/00100/2020, UIDP/00100/2020, UIDB/00313/2020 and UIDP/00313/2020 and IMS - LA/P/0056/2020.

M.C.M. Sequeira acknowledges the PhD grant funded by FCT ref. UI/BD/152239/2021.



IST-ID
Associação do Instituto Superior Técnico
para a Investigação e Desenvolvimento

fct
Fundação
para a Ciência
e a Tecnologia